International Journal of Smart Grid and Clean Energy

Optimal operation of integrated electrical, district heating and natural gas system in wind dominated power system

Ana Turk, Qing Zeng, Qiuwei Wu, Arne Hejde Nielsen

Department of Electrical Engineering, Technical University of Denmark, 2800 Kongens Lyngby, Denmark

Abstract

Nowadays, installed capacity of renewable energy sources is increasing at a high rate and even higher increase is expected in the future. In order to accommodate renewable energy sources, integration of gas, electricity and district heating network is a promising solution. This paper provides a coordinated operation and analysis of electricity, district heating and natural gas system with integrated wind farm. The interactions among different energy sectors will provide more flexibility required by the future renewable energy system. A nonlinear optimization problem is presented with focus on decreasing the operational cost and improving efficiency of integrated system, as well as meeting the demands. Optimal operation is performed for a test case system including constraints of individual systems and linkages between each of the systems. The test system includes electrical, district heating and natural gas subsystem with thermal and gas storages, combined heat and power and power to gas units and wind turbine. Simulation results show that integration of electricity, heating and natural gas system decreases the operational cost and provides higher flexibility to the system. Moreover, wind curtailment is reduced with integration of P2G.

Keywords: Combined heat and power, electrical system, district heating system, natural gas system, optimal dispatch, power to gas

1. Introduction

Long-term targets for 2020, 2030 and 2050 for European countries are introduced by European Commission with the main target of having a sustainable and secure energy system by 2050. Taking Denmark as example, in 2015, wind power penetration was 50% and in 2014, wind power generation exceeded demand by almost 1000 h. Danish main goal by 2050 is 100% renewable energy sources (RES) based system [1]. Nowadays, the installed capacity of RES is increasing at a high rate and replacing conventional generators. Consequently, mismatch between generation and demand can occur, leading to unstable system. In order to realize the long-term goal of RES based systems operating in a secure, reliable and economic manner, the synergy between electricity, heat and gas has to be explored [2].

Extensive studies have been carried out related to integration of energy storages and flexible loads in order to accommodate the RES including [3]. Furthermore, electric water heater, combined heat and power (CHP) and heat pumps are widely used and an extensive literature can be found for linkage between electrical power system (EPS) and district heating system (DHS). In [4], the optimal dispatch of EPS and DHS of urban area with increased RES is performed with the aim to decrease operational costs of both systems. Authors of [7] introduced and compared two methods, decomposed and integrated, for combined analysis of EPS and DHS where optimal dispatch of EPS is considered only. Optimization of operation of DHS with thermal storage in pipelines is presented in [8] and optimization of supply temperature and mass flow rate in DHS with minimization of operational cost and losses is presented in [9]. When it comes to natural gas system (NGS) and EPS, basic principle of modelling of NGS, and optimal power flow of EPS and NGS is presented in [10]. Moreover, the link between NGS and EPS used

* Manuscript received September 10, 2019; revised January 8, 2020.
Corresponding author. Tel.: +45-45-25-35-29; *E-mail address*: qw@elektro.dtu.dk.
doi: 10.12720/sgce.9.2.237-246

to accommodate RES is power to gas (P2G) unit which has a fast response to changes in generation and demand according to [5, 6]. Furthermore, it can convert excess electricity from RES to hydrogen or methane which further on can be stored in gas pipeline or storage for longer periods [5]. The interaction of NGS and EPS through P2G units is studied in [11]. Steady state analysis of NGS and EPS system with units P2G and CHP is presented in [5]. Based on the work done in mentioned papers, the interactions among different energy sectors should provide higher flexibility required by the future RES system while minimizing the operational costs and losses. One of the prominent solutions to balance the renewable production and increase flexibility would be to integrate EPS, DHS and NGS with energy storages and coupling components. In this paper multi period optimal operation focused on minimizing operational costs of all systems and detailed constraints of integrated network are presented. Firstly, mathematical models are used to describe the DHS including demand, thermal storage and heating source like CHP units. In DHS, temperature of water is important parameter that must be maintained within permissible operational limits and the effect of water temperature on DHS is further on explained in Section 2.2. Secondly, mathematical model of NGS including gas source, P2G unit and gas storage is developed. Finally, integration of EPS, DHS and NGS including their components and links, and analysis of interactions between electricity, gas and heat is conducted. Further on, optimal operation strategy of integrated energy system is developed. Optimal operation including mathematical models is performed in software General Algebraic Modeling System (GAMS) and results are additionally verified through MATLAB Yalmip toolbox and MATPOWER toolbox.

This paper is organized as follows. The second section introduces the mathematical modelling of EPS, DHS and NGS. Accordingly, linking components of integrated system are presented with corresponding constraints. In section three, test case of integrated system is presented and analysed. The section four provides the results of the test case system and in section five the conclusion of this work is given.

1.1. Nomenclature

Notation	Description	Unit
$\Lambda^{EPS/DHS/NGS}$	Set of nodes in EPS/DHS/NGS	
$\Omega_n^{ED/WT}$	Set of electricity demands/wind turbines at node *n*	
$\Omega_n^{HL/HS/CHP}$	Set of heat demands/ /heat storages/CHP at node *n*	
$\Omega_n^{GS/GD/GC/P2G/ST}$	Set of gas sources/gas demands/GC/P2G/gas storages at node *n*	
T	Set of hours	
$\alpha_j, \beta_j, \gamma_j$	Cost coefficients for CHP	\$/MWh
$\lambda_{mn,t}$	Thermal conductivity of pipe m-n	W/m ℃
λ_g^{GC}	Operational energy consumption coefficient of GC *g*	
η^{GC}	Compression efficiency of GC *g*	
$\eta_j^{\mathrm{e}}, \eta_j^h$	Generating electrical and thermal efficiency of CHP unit *j*	
η_k^{P2G}	The energy conversion efficiency of at P2G unit	
$\tau_{mn,t}^{\mathrm{in}}$	Temperature of inlet to node n of pipe m-n	℃
$\tau_{mn,t}^{out}$	Temperature of outlet of node m of pipe m-n	℃
$\tau_{mn,t}^{\mathrm{in/out,min/max}}$	Minimum/maximum water temperature of inlet/outlet of pipe *m-n*	℃
c	Specific heat capacity of water	J/kg ℃
c_k, CR	Specific heat ratio for natural gas and compression ratio	
C^{CHP}, C^{GS}, C^{P2G}	Marginal cost of power and gas supply: CHP, gas source and P2G	\$/MWh
$C^{HST,in/out}$	Marginal cost of heat input/output to/from heat storage	\$/MWh
$C^{GST,in/out}$	Marginal cost of gas input/output to/from gas storage	\$/MWh

C_t	Total operational cost of integrated system	\$/h
$D_{j,t}^{\mathrm{CHP}}$, $D_{k,t}^{P2G}$	Gas consumption in CHP unit *j* and power demand in P2G unit *k*	MW
$D_{g,t}^{\mathrm{GC}}$, $D_{d,t}^{\mathrm{GD}}$, $D_{e,t}^{ED}$	Gas consumption in GC *g*, gas demand and electric demand	MW
E^{GC}	GC parasitic efficiency	
$G_{nm,t}$	Gas flow rate in pipeline *n-m*	m^3/h
H_j^{CHP} , $H_j^{CHP,\min/\max}$	Heat supply and max/min heat supply from CHP unit j	MW
$H_{h,t}^{HS,in}$	Heat output of heat storage h to heat network,	MW
$H_{h,t}^{HS,out}$	Heat output of heat network to heat storage h	MW
$H_{l,t}^{HL}$	Heat demand	MW
$H_h^{HS,in/out,\min/\max}$	Minimum/maximum heat input/output capacity of heat storage h	MW
$HS_{h,t}$, $HS_h^{\min/\max}$	Heat stocks and max/min heat reserve in heat storage h	MWh
K^{GC}	Constant of GC	
LHV	Lower heating value	MJ/m^3
l_{mn}	Length of district heating pipe m-n	m
$m_{mn,t}$, $m_{mn,t}^{\max/\min}$	Water flow rate and max/min water flow rate in pipe m-n	kg/s
$p_{n,t}^2$, $(p_{n,t}^2)^{\min/\max}$	Gas pressure of node n and minimum/maximum operating limits	MPa^2
$P_{j,t}^{\mathrm{CHP}}$	Power supply from CHP unit *j*	MW
$P_{WT,t}$, $P_{WT,t}^{\mathrm{spill}}$	Power output of wind unit *f* and power spillage for wind unit *f*	MW
P_G , Q_G , P_D , Q_D	Active and reactive - output power of generator and load power	MW, MVAr
$P_G^{\min/\max}$, $Q_G^{\min/\max}$	Upper and lower bound of active and reactive output power	MW, MVAr
$Q_{g,t}^{\mathrm{GS}}$, $Q_g^{\mathrm{GS,min/max}}$	Gas supply and minimum/maximum gas supply from gas source	MW
$Q_{k,t}^{\mathrm{P2G}}$, $Q_k^{\mathrm{P2G,min/max}}$	Gas supply and minimum and maximum level from P2G unit *k*	MW
$Q_{s,t}^{\mathrm{ST,in/out}}$, $Q_s^{\mathrm{ST,in/out,max}}$	Gas input/output and gas input/output capacity of gas storage *s*	MW
$S_{nm,t}$, $S_{nm}^{\max}$	Gas flow rate and transmission capacity of gas pipeline *n-m*	MW
$S_{g,t}^{\mathrm{GC}}$	Gas flow rate through gas compressor *g*	MW
$ST_{s,t}$, $ST_s^{\min/\max}$	Gas stocks and minimum/maximum gas stock in gas storage *s*	MWh
T_s , Z_{a}	Suction temperature of GC and average compressibility factor	ℜ, -
$V, V^{\min,\max}, \delta$	Voltage amplitude, voltage amplitude limits, phase angle of bus n	kV, rad
Y_{mn}	Admittance of transmission line *n-m*	p.u.
Z_{nm}	Resistance coefficient of the pipeline	$kPa^2/(MW)^2$

2. Mathematical Modeling

2.1. Modeling of electric power system

Optimal power flow studies have been performed for a long time where the main objective is to supply the load reliably and as economically as possible. The power flow study in this work is optimal AC power flow. The goal of this study is to obtain generators active and reactive power and voltage angle and magnitude on each bus. Active and reactive power flow balance equations for every bus in the EPS in the

form of equality constraints are shown in (1)-(2) with the operational limits of the variables in (3)-(4) [12]. To further on expand the power flow balance equation regarding CHP, P2G and wind turbine, (5) is presented with its operational constraint in (6).

$$P_{Gi} - P_{Di} = |V_i| \sum_{j=1}^{n} |V_i| |Y_{ij}| \cos(\delta_i - \delta_j - \theta_{ij}) \tag{1}$$

$$Q_{Gi} - Q_{Di} = |V_i| \sum_{j=1}^{n} |V_i| |Y_{ij}| \sin(\delta_i - \delta_j - \theta_{ij}) \tag{2}$$

$$P_{Gi}^{\min} \le P_{Gi} \le P_{Gi}^{\max} \tag{3}$$

$$V_i^{\min} \le V_i \le V_i^{\max} \tag{4}$$

$$\begin{aligned} &\sum_{i \in \Omega_n^{\mathrm{CHP}}} P_{j,t}^{CHP} + \sum_{f \in \Omega_n^{\mathrm{WF}}} \left(P_{WT,t} - P_{WT,t}^{\mathrm{spill}} \right) - \\ &- \sum_{k \in \Omega_n^{\mathrm{P2G}}} D_{P2G,k,t} - \sum_{e \in \Omega_n^{\mathrm{ED}}} D_{e,t}^{\mathrm{ED}} = \sum_{m \in \Omega_n} |V_n| |V_n| |Y_{nm}| \cos(\delta_n - \delta_m - \theta_{nm}), \qquad \forall t \in T, \forall n \in \Lambda^{\mathrm{EPS}} \end{aligned} \tag{5}$$

$$0 \le P_{WT,t}^{\mathrm{spill}} \le P_{WT,t}, \quad \forall f \in \Omega^{\mathrm{WT}}, \forall t \in T \tag{6}$$

2.2. Modeling of district heating system

DHS consists of supply pipelines delivering heat from the heat source to the heat demand and return pipelines coming back to the heat source. As previously mentioned in Section 1, temperature of water is important parameter. The supply temperature varies from 70 ℃ to 120 ℃, while return temperature is lower depending on the heat extracted by the heat load [7]. DHS model consists of hydraulic and thermal model. Variable in hydraulic model is mass flow, while thermal model includes supply and return temperatures and heat power delivered by the heat source. Hydraulic equation presenting continuity of flow demonstrates that the mass flow entering the node equals to the mass flow leaving the node and mass flow consumption at that node as shown in (7). Thermal model consists of nodal heat balance equation, temperature drop and temperature mix equations. Heat balance of DHS consisting of heat source, heat load and storage is presented in (8). The heat power being positive means releasing power to the system, while negative indicates heat loss or heat being consumed by the load. Further on, the equation for temperature drop is provided in (9) where λ depends on diameter and heat transfer coefficient of the pipeline. In this work a constant of 0.4 is taken for λ. The heat loss of each pipeline is due to the heat transfer along the pipe from high water temperature to the ambient temperature. In this work ambient temperature of 10 ℃ is chosen. The total heat loss of DHS is the sum of the heat losses in each pipeline. The temperature drop equation is applicable for both supply and return network. Furthermore, temperature mix equation shown in (10) is used when there is more than one incoming mass flow to the node. The temperature of mass flow going out of the node is then calculated based on the temperatures of incoming mass flows [7]. The operational limits for DHS and heat storage balance equation are presented in (11)-(16). Lower and upper temperature limits for DHS in this work are 30 ℃ and 80 ℃ respectively. As mentioned, DHS has storages to optimize electricity and heat production. Meaning, in cases of overproduction, CHP decreases its generation and while heating demand is high, the heat is provided by the heat storage.

$$\sum_{m \in \Lambda_n} m_{mn,t} = 0, \forall m, n \in \Lambda^{\mathrm{DHS}}, \forall t \in T \tag{7}$$

$$\sum_{j\in\Omega_n^{\mathrm{CHP}}} H_{j,t}^{\mathrm{CHP}} + \sum_{s\in\Omega_n^{\mathrm{HS}}} \left(H_{s,t}^{\mathrm{HS,in}} - H_{s,t}^{\mathrm{HS,out}}\right) - \sum_{l\in\Omega_n^{\mathrm{HL}}} H_{l,t}^{\mathrm{HL}} = c\cdot m_{mn,t}\cdot\left(\tau_{mn,t}^{in} - \tau_{mn,t}^{out}\right), \quad \forall m,n\in\Lambda^{\mathrm{DHS}}, \forall t\in T \tag{8}$$

$$\tau_{mn,t}^{in} - \tau_{mn,t}^{\mathrm{a}} = e^{\frac{-\lambda_{mn,t}L_{mn}}{cm_{mn,t}}}\left(\tau_{mn,t}^{out} - \tau_{mn,t}^{\mathrm{a}}\right), \forall m,n\in\Lambda^{\mathrm{DHS}}, \forall t\in T \tag{9}$$

$$\tau_{mn,t}^{out}\sum_{m\in\Lambda_n} m_{mn,t} = \sum_{m\in\Lambda_n}\left(m_{nm,t}\cdot\tau_{nm,t}^{in}\right), \forall m,n\in\Lambda^{\mathrm{DHS}}, \forall t\in T \tag{10}$$

$$H_j^{\mathrm{CHP,min}} \le H_{j,t}^{\mathrm{CHP}} \le H_j^{\mathrm{CHP,max}}, \quad \forall j\in\Omega^{\mathrm{CHP}}, \forall t\in T \tag{11}$$

$$HS_{h,t+1} = HS_{h,t} + \left(H_{h,t}^{\mathrm{HS,out}} - H_{h,t}^{\mathrm{HS,in}}\right), \quad \forall h\in\Omega^{\mathrm{HS}}, \forall t\in T \tag{12}$$

$$H_h^{\mathrm{HS,in/out,min}} \le H_{h,t}^{\mathrm{HS,in/out}} \le H_h^{\mathrm{HS,in/out,max}}, \quad \forall h\in\Omega^{\mathrm{HS}}, \forall t\in T \tag{13}$$

$$HS_h^{\min} \le HS_{h,t} \le HS_h^{\max}, \quad \forall h\in\Omega^{\mathrm{HS}}, \forall t\in T \tag{14}$$

$$m_{mn}^{\min} \le m_{mn,t} \le m_{mn,t}^{\max}, \forall m,n\in\Lambda^{\mathrm{DHS}}, \forall t\in T \tag{15}$$

$$\tau_{mn}^{\mathrm{in/out,min}} \le \tau_{mn,t}^{\mathrm{in/out}} \le \tau_{mn}^{\mathrm{in/out,max}}, \forall m,n\in\Lambda^{\mathrm{DHS}}, \forall t\in T \tag{16}$$

2.3. Modeling of natural gas system

NGS consists of loads, pipes, gas compressors (GC), storages and P2G plants. While natural gas is being transported, there is a gas pressure loss due to the pipeline and gas friction and energy loss due to the heat transfer between gas and environment along pipelines. Therefore, compressors are integrated in the system to compensate for the losses and to keep the gas flowing. In that way, a part of transported gas is used to power the compressors. Other than gas source supply, P2G units are integrated which are using surplus electricity to produce hydrogen. For modelling purposes of NGS, following equations are being used. Firstly, (17) is pipeline flow equation with fixed gas pressure at reference node to 1MPa each hour. Secondly, nodal gas flow balance is shown in (18). Further on, in (19) energy consumption by GC is provided. Balance of gas storage is shown in (20) and operational limits of NGS variables are presented in (21)-(26).

$$p_{n,t}^2 - p_{m,t}^2 = Z_{nm}\left(S_{nm,t}\right)^2, \quad \forall n,m\in\Lambda^{\mathrm{NGS}}, \forall t\in T \tag{17}$$

$$\begin{aligned}&\sum_{g\in\Omega_n^{\mathrm{GS}}} Q_{g,t}^{\mathrm{GS}} + \sum_{s\in\Omega_n^{\mathrm{ST}}}\left(Q_{s,t}^{\mathrm{ST,out}} - Q_{s,t}^{\mathrm{ST,in}}\right) + \sum_{k\in\Omega_n^{\mathrm{P2G}}} Q_{k,t}^{\mathrm{P2G}}\\ &- \sum_{d\in\Omega_n^{\mathrm{GD}}} D_{d,t}^{\mathrm{GD}} - \sum_{g\in\Omega_n^{\mathrm{GC}}} D_{g,t}^{\mathrm{GC}} - \sum_{j\in\Omega_n^{\mathrm{CHP}}} D_{j,t}^{\mathrm{CHP}} = \sum_{m\in\Lambda_n} S_{nm,t}, \quad \forall m,n\in\Lambda^{\mathrm{NGS}}, \forall t\in T\end{aligned} \tag{18}$$

$$D_{g,t}^{\mathrm{GC}} = \lambda_g^{\mathrm{GC}} S_{g,t}^{\mathrm{GC}} = K^{\mathrm{GC}} Z_{\mathrm{a}}\left[\frac{T_s}{E^{\mathrm{GC}}\eta^{\mathrm{GC}}}\right]\left[\frac{c_k}{c_k - 1}\right]\left[\left(CR\right)^{\frac{c_k-1}{c_k}} - 1\right] S_{g,t}^{\mathrm{GC}}, \quad \forall g\in\Omega^{\mathrm{GC}}, \forall t\in T \tag{19}$$

$$ST_{s,t} = ST_{s,0} + \sum_{t=1}^{t}\left(Q_{s,t}^{\mathrm{ST,in}} - Q_{s,t}^{\mathrm{ST,out}}\right), \forall s\in\Omega^{\mathrm{ST}}, \forall t\in T \tag{20}$$

$$Q_g^{\mathrm{GS,min}} \le Q_{g,t}^{\mathrm{GS}} \le Q_g^{\mathrm{GS,max}}, \quad \forall g\in\Omega^{\mathrm{GS}}, \forall t\in T \tag{21}$$

$$Q_k^{\mathrm{P2G,min}} \le Q_{k,t}^{\mathrm{P2G}} \le Q_k^{\mathrm{P2G,max}}, \quad \forall k \in \Omega^{\mathrm{P2G}}, \forall t \in T \tag{22}$$

$$0 \le Q_{s,t}^{\mathrm{ST,in/out}} \le Q_s^{\mathrm{ST,in/out,max}}, \quad \forall s \in \Omega^{\mathrm{ST}}, \forall t \in T \tag{23}$$

$$(p_{n,t}^2)^{\min} \le p_{n,t}^2 \le (p_{n,t}^2)^{\max}, \quad \forall n \in \Lambda^{\mathrm{NGS}}, \forall t \in T \tag{24}$$

$$-S_{nm}^{\max} \le S_{nm,t} \le S_{nm}^{\max}, \quad \forall m,n \in \Lambda^{\mathrm{NGS}}, \forall t \in T \tag{25}$$

$$ST_s^{\min} \le ST_{s,t} \le ST_s^{\max}, \quad \forall s \in \Omega^{\mathrm{ST}}, \forall t \in T \tag{26}$$

In order to obtain MW as unit for gas flow, as presented in notation, conversion from m^3/h to MW must be performed. The equation is presented in (27) and the reason for that is as follows. During combustion process of hydrocarbon fuel, a water is released as by-product. The generated heat in water vapour cannot be recovered and due to that lower value of heating power, LHV is used [5, 13]. LHV considered in this work is 37.26 MJ/m^3 according to [5].

$$S_{nm,t} = G_{nm,t} \frac{LHV}{3600} \tag{27}$$

Moreover, the unit of energy consumption in GC in (19) is horsepower (HP) and conversion from HP to MW must be done. Firstly, m^3/h must be converted to million standard cubic feet per day (MMSCFD) where 1 m^3/h equals to $8.47 \cdot 10^{-4}$ MMSCFD in order to obtain HP. Lastly, 1 HP equals to $746 \cdot 10^{-6}$ MW.

2.4. Modeling of coupling components – combined heat and power and power to gas

There are two linking components in this work, CHP and P2G. CHP is consuming natural gas for generating electricity, where a byproduct is heat used for DHS. Therefore, a relationship between electricity and heat generation can be obtained. Moreover, gas consumption of CHP unit based on electricity and heat generation can be calculated as shown in (28)-(29). The η^{e} and η^{h} in this work are set to 0.3 and 0.5 respectively [14].

$$P_{j,t}^{\mathrm{CHP}} = D_{j,t}^{\mathrm{CHP}} \eta_j^{\mathrm{e}}, \quad \forall j \in \Omega^{\mathrm{CHP}}, \forall t \in T \tag{28}$$

$$H_{j,t}^{\mathrm{CHP}} = D_{j,t}^{\mathrm{CHP}} \eta_j^{h}, \quad \forall j \in \Omega^{\mathrm{CHP}}, \forall t \in T \tag{29}$$

P2G is a unit converting electricity to hydrogen using electrolysis or methane through methanation process. The hydrogen can be used as fuel in industrial and transport sector, while methane can be used in all natural gas pipelines and for meeting gas demand [2]. The energy necessary for obtaining hydrogen is lower than for obtaining methane according to [15]. Therefore, in this work, methanation process is considered which is leading to lower efficiency of P2G of 0.5. The relationship between gas production and consumed electricity of P2G is shown in (30).

$$Q_{k,t}^{\mathrm{P2G}} = \eta_k^{\mathrm{P2G}} D_{k,t}^{\mathrm{P2G}}, \quad \forall k \in \Omega^{\mathrm{P2G}}, \forall t \in T \tag{30}$$

2.5. Objective function

The objective is to perform optimal dispatch which is allocating generation among every generation unit and storage maintaining the total cost minimized. Therefore, the objective function is shown in (31).

$$\begin{aligned} C_t = \min \sum_{t=1}^{n^{\mathrm{T}}} \Bigg\{ \sum_{j=1}^{n_g} \alpha_j + \beta_j P_j^{CHP} + \gamma_j (P_j^{CHP})^2 + \sum_{h=1}^{n^{CHP}} \left(C_h^{CHP} H_{h,t}^{\mathrm{CHP}} \right) + \sum_{s=1}^{n^{HS}} \left(C_s^{\mathrm{HST,in}} H_{s,t}^{\mathrm{HS,in}} + C_s^{\mathrm{HST,out}} H_{s,t}^{\mathrm{HS,out}} \right) \Bigg\} \\ + \sum_{t=1}^{n^{T}} \Bigg\{ \sum_{g=1}^{n^{\mathrm{GS}}} C_g^{\mathrm{GS}} Q_{\mathrm{g},t}^{\mathrm{GS}} + \sum_{s=1}^{n^{\mathrm{ST}}} \left(C_s^{\mathrm{GST,in}} Q_{s,t}^{\mathrm{ST,in}} + C_s^{\mathrm{GST,out}} Q_{s,t}^{\mathrm{ST,out}} \right) + \sum_{k=1}^{n^{P2G}} C_k^{P2G} Q_{k,t}^{P2G} \Bigg\} \end{aligned} \tag{31}$$

3. Integrated Electricity, District Heating and Natural Gas Test Case System

Test case of integrated 4-bus EPS, 6-node DHS and 5-node NGS is presented in Fig. 1. Electricity, heat and gas demand and wind power generation data are provided by Danish transmission system operator, Energinet. Time interval of obtained data is 1 h and simulation period of 1 day is chosen in January. The data is converted in per unit system where base values of power and gas pressure are 1 MW and 1 MPa respectively. Additional data for test system is presented in Table 1 and Table 2 according to [4, 5, 6]. The operation of integrated test case model is solved by solver IPOPT in GAMS.

Table 1. Values and limits of variables and parameters

Parameter/Variable	Value
$(H_j^{\mathrm{CHP}}, H_h^{\mathrm{HS,in/out}}, Q_k^{\mathrm{P2G}}, Q_g^{\mathrm{GS}})^{\min}$	0 pu
$HS_h^{\min}, ST_s^{\min}, H_j^{\mathrm{CHP,max}}, Q_g^{\mathrm{GS,max}}$	0.1 pu, 0.1 pu, 1 pu, 7.7 pu
$(Q_k^{\mathrm{P2G}}, H_h^{\mathrm{HS,in/out}}, Q_s^{\mathrm{ST,in/out}})^{\max}$	0.1 pu, 0.1pu, 0.1pu
$m_{mn}^{\min}, m_{mn}^{\max}$	1 kg/s, 3 kg/s
$HS_{h,t}^0, ST_{s,t}^0, HS_h^{\max}, ST_s^{\max}$	0.5, 0.5, 0.9, 0.9
Y_{nm}, T_s	0.09+0.1577j, 530 ℜ
$Z_a, \eta^{\mathrm{GC}}, E^{\mathrm{GC}}, K^{\mathrm{GC}}, c_k, CR$	0.95,0.85,0.99,0.0854,1.3,1.414
$L_{12}, L_{23}, L_{65}, L_{54}$	400, 300, 200, 300 m
$Z_{12}, Z_{23}, Z_{34}, Z_{35}$	0.0280, 0.0373, 0.0186, 0.0202
$V^{\min}, V^{\max}, P^{CHP,\min}, P^{CHP,\max}$	0.95, 1.05, 0, 1

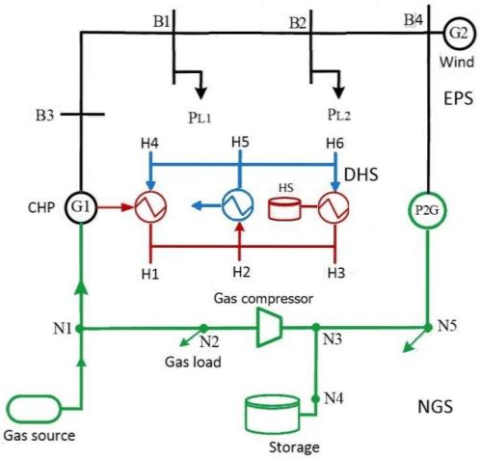

Fig. 1. Test case of integrated EPS, DHS and NGS.

Table 2. Values of marginal cost of each generating unit and storage

Parameter	α_j	β_j	γ_j	C_h^{CHP}	$C_s^{HST,in}$	$C_s^{HST,out}$	C_g^{GS}	$C_s^{GST,in}$	$C_s^{GST,out}$	C_k^{P2G}
Marginal Cost ($/MWh)	50	13	0.2	4	2	16	8	10	2	2

4. Results of Optimal Operation of Integrated System

In Fig. 2.a) optimal generation of EPS based on lowest operational cost is shown. Generation is including active output power of wind turbine and CHP, while demand is including electricity demand of EPS and electricity consumed by P2G for electrolysis and methanation process. As it can be noticed, in moments of surplus power of wind turbine, P2G uses excess electricity and converts it to gas. The wind

power production is the highest in the morning and evening and accordingly the overall demand is higher that period due to electricity consumption of P2G. Accordingly, there is a wind spillage from 0.025pu - 0.1pu for the last four hours of the day. By considering higher limit of gas supply from P2G, as example 0.2pu, the wind spillage would be zero. Therefore, it can be observed that the optimal operation of EPS is obtained. Optimal operation of DHS generation and thermal demand are shown in Fig. 2.b). Heat demand is including only heat load (red curve), while blue curve is showing heat demand and losses. Thermal loss during 24 hours is 10.3%. In this work, the heat is provided by CHP and heat storage. The heat provided by heat storage is almost constant during entire day. Therefore, the storage balance is dropping as seen in Fig. 3.b). Initial value of the heat storage state is 0.5, where at the end of the day decreases to 0.167. It is not reaching the minimum permitted limit of the storage capacity by the end of the day.

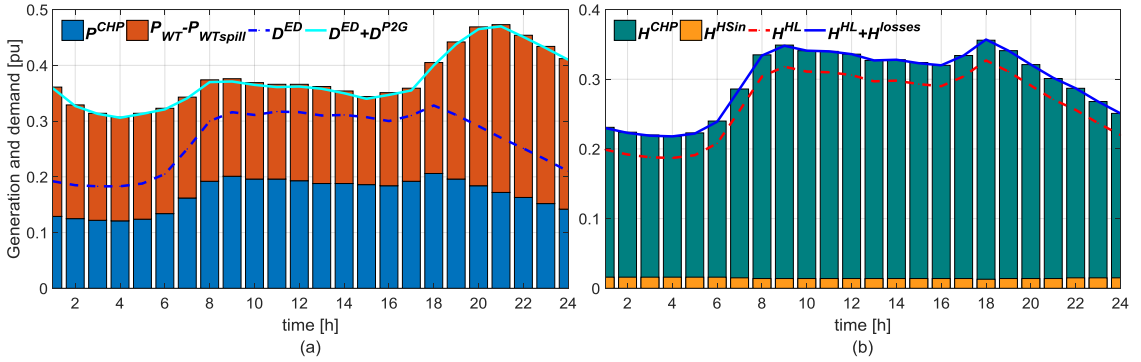

Fig. 2. Generation and demand: (a) EPS (b) DHS.

The results of optimal operation of generation and demand of NGS are shown in Fig. 3.a). The gas supply consists of gas source, P2G and gas storage supply while the entire demand (black curve) is gas load and gas consumption of CHP. It can be seen that P2G is supplying higher amount of gas at the moments of higher excess electricity from wind turbines. Accordingly, the gas storage is supplying the gas. The initial value of gas storage capacity is 0.5, and at the end of the day is reaching its 0.1 as seen in Fig. 3.b). Both, heat and gas storage are effected by EPS. Heat provided by CHP is high during entire day resulting in almost constant heat supply by heat storage. When it comes to NGS, due to the high wind production at the last four hours of the day, P2G is reaching its maximum available gas supply of 0.1pu as seen in Fig. 3a). In that period, gas storage increases its output reaching maximum permitted output in order to maintain cost effective system. The behavior can be observed in Fig. 3b) where indication of increase of gas storage output is observed after intersection of both curves.

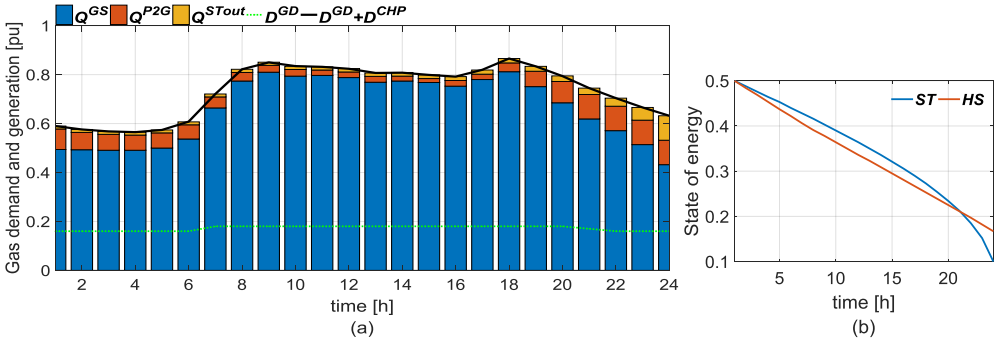

Fig. 3. Results: (a) Generation and demand of NGS (b) State of energy of heat and gas storage.

Water temperature of the each node in DHS is presented in Fig. 4.a). The temperatures of node 1 and node 6 are the highest since the heat source and heat storage are connected to that nodes respectively and the heat is supplied to the grid. The temperature after the heat is being consumed by the load is lower than temperature at node 5. Therefore, temperature of the node 5 corresponds to the mix of incoming

temperature from load and incoming temperature of 80 ℃ from node 6. Accordingly, a decrease in temperature at node 4 is seen due to the losses caused by a difference between water temperature in the pipes and ambient temperature. The same can be observed for node 2 and node 3. Accordingly, by looking at the heat demand profile in Fig. 2.b), it can be noticed that temperature at node 5 is decreasing in moment of heat load increase. When it comes to gas pressure in the NGS, it is maintained within secure limits and the behavior is similar as temperature behavior in DHS. With higher gas demand, the gas pressure drops. Fig.4.b) is showing gas flow rate in NGS in each pipe. The positive gas flows for some hours have pipe 12, pipe 23 and pipe 35. Opposite flow is present in pipe 34 entire day. Meaning, loads at node 5 and node 2 are additionally supplied by gas storage and P2G in moments of high wind turbine power output. The opposite flow along the pipe 34 is due to the gas provided by gas storage to the system.

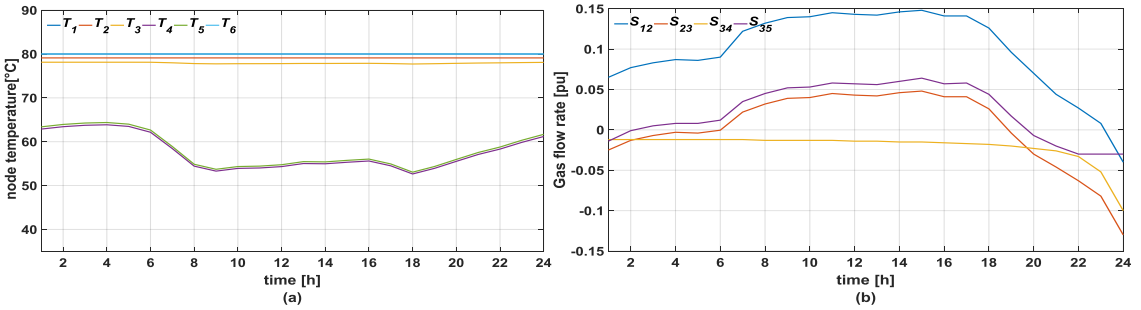

Fig. 4. Results: (a) Temperature at nodes in DHS (b) Gas flow rate in pipelines in NGS.

5. Conclusion

This paper investigates a coordination between EPS, DHS and NGS and provides an optimal operation of an integrated system with the objective to minimize total operational cost of all three systems. For simulation purposes, a test case model consisting of CHP providing heat and electricity, gas source, P2G, wind turbines and heat and gas storages is used. Mathematical modelling of EPS, DHS and NGS with its coupling components is performed and the integrated model with its constraints is solved in GAMS. Simulation results show that integration of EPS, DHS and NGS with linking components provides a flexibility to the system in a way that reduces fuel consumption and fluctuations due to the wind variable output power. Accordingly, outcome of this work shows that excess electricity can be converted to gas through P2G unit and, therefore, wind curtailment can be reduced. To conclude, integration of EPS, DHS and NGS is a prominent solution for providing flexibility to the power system.

Conflict of Interest

The authors declare no conflict of interest.

Author Contributions

A.T. designed and modelled the system, conducted research, analyzed the data and co-wrote the paper. Q.Z. provided the data, analyzed the data and co-wrote the paper. Q.W. supervised the research, analyzed the data, and co-wrote and revised the paper. A.H.N. supervised the research and co-wrote the paper. All authors had approved the final version.

References

[1] Danish energy agency (August 2018): Danish climate policies," [Online]. Available: https://ens.dk/en/our-responsibilities/energy-climate- politics/danish-climate-policies

[2] European Power to Gas (September 2017): White Paper on power-to-gas published by European Power to Gas Platform,

[Online]Available:http://www.europeanpowertogas.com/media/files/European%20Power%20to%20Gas_White%20Paper.pdf.
[3] Turk A, Sandelic M, Pillai RJ, Chaudhary S. Frequency control with flexible demand and storages to support large Renewable energy generation. In: *Proc. of 18th EEEIC*, 2018
[4] Li J, Fang J, Zeng Q, Chen Z. Optimal operation of the integrated electrical and heating systems to accommodate the intermittent renewable sources. *Journal of Applied Energy*, 2016;167: 244-254
[5] Zeng Q, Fang J, Li J, Chen Z. Steady-state analysis of the integrated natural gas and electric power system with bi-directional energy conversion. *Journal of Applied Energy*, 2016; 184: 1483-1492
[6] Zeng Q, Zhang B, Fang J, Chen Z. A bi-level programming for multistage co-expansion planning of the integrated gas and electricity system. *Journal of Applied Energy*, 2017; 200: 192-203
[7] Liu X, Wua J, Jenkins N, Bagdanavicius A. Combined analysis of electricity and heat networks. *Journal of Applied Energy*, 2016;162:1238-1250.
[8] Bujalski W, Lesko M. Modeling of district heating networks for the purpose of operational optimization with thermal energy storage. Research Report. Warsaw University of Technology Institute of Heat Engineering, Warszawa, Poland, 2017.
[9] Pirouti M, Bagdanavicius A, Wu J, Ekanayake J. Optimisation of supply temperature and mass flow rate for a district heating network. In: *Proc. of ECOS 2012*, 2012:1–12
[10] Seungwon A, Li Q, Gedra TW, Natural gas and electricity optimal power flow. Presented at: 2003 IEEE PES Transmission and Distribution Conference and Exposition
[11] Yang Z, Gao C, Zhang J. The interaction of gas and electricity hybrid energy internet. Presented at 2017 IEEE Conference on Energy Internet and Energy System Integration (EI2)
[12] Frank S, Rebennack S. An introduction to optimal power flow: Theory, formulation, and examples. In: IIE Transactions, 2016; 48(12), 1172-1197
[13] Beér JM. High efficiency electric power generation: The environmental role. In Progress in Energy and Combustion Science, 2007:33(2):107-134
[14] Eurostat (May 2017): Combined heat and power (CHP) generation,[Online]. Available: https://ec.europa.eu/eurostat /documents/38154/42195/Final_CHP_reporting_instructions_reference_year_2016_onwards_30052017.pdf
[15] Lehner M, Tichler R, Steinmuller H, Koppe M. Power-to-Gas: Technology and Business Models, Springer, 2014

Copyright © 2020 by the authors. This is an open access article distributed under the Creative Commons Attribution License (CC BY-NC-ND 4.0), which permits use, distribution and reproduction in any medium, provided that the article is properly cited, the use is non-commercial and no modifications or adaptations are made.